Overlapping Substrate and Inhibitor Specificity of Human and Murine ABCG2

Joshua Bakhsheshian, Matthew D. Hall, Robert W. Robey, Michelle A. Herrmann, Jin-Qiu Chen, Susan E. Bates, Michael M. Gottesman

Laboratory of Cell Biology (J.B., M.D.H., M.M.G.); Cancer Therapeutics Branch (R.W.R., S.E.B.); Collaborative Protein Technology Resource (J.-Q.C., M.A.H.), Center for Cancer Research, National Cancer Institute, National Institutes of Health, Bethesda, MD, USA

Running Title: Functional comparison of human and murine ABCG2

Address correspondence to: Michael M. Gottesman, Laboratory of Cell Biology, National Cancer Institute, National Institutes of Health, 37 Convent Drive, Rm. 2108, Bethesda, MD 20892. Phone: 301-496-1530; Fax: 301-402-0450; E-mail: mgottesman@mail.nih.gov

Number of text pages: 20
Number of tables: 2
Number of figures: 4
Number of references: 53
Number of words in:
Abstract: 232
Introduction: 621
Discussion: 1024

Abbreviations

ABC, ATP-binding cassette; ABCG2, ATP-binding cassette sub-family G member 2; BCRP, Breast cancer resistance protein; P-gp, P-glycoprotein; Pp-18, purpurin-18; MRP1, Multidrug resistance protein 1; MPPa, pyropheophorbide a methyl ester; Estradiol, 17-β-estradiol; FTC, fumitremorgin C; ATPase, Adenosine triphosphatase.

DMD Fast Forward. Published on July 18, 2013 as DOI: 10.1124/dmd.113.053140
This article has not been copyedited and formatted. The final version may differ from this version.

Abstract

ABCG2 (also known as breast cancer resistance protein; BCRP) is an ATP-binding cassette (ABC) transporter localized to the plasma membrane where it mediates the efflux of xenobiotics, including potential therapeutics. Studies investigating Abcg2 function at the blood-brain-barrier in mouse models are often compared to human ABCG2 function. It is critical to understand the nature of species differences between mouse and human ABCG2, since extrapolations are made from murine data to humans. Two independent drug-selected cell line pairs expressing human or mouse ABCG2 were compared for efflux of fluorescent substrates using flow cytometry. To this end, we developed and characterized a new mouse Abcg2-expressing subline that demonstrated efflux of known fluorescent ABCG2 substrates and increased resistance to mitoxantrone, which is reduced in the presence of the ABCG2 inhibitor Ko143. Our results indicate that the substrate specificity of human and mouse ABCG2 is very similar. We identified a new human and mouse ABCG2 substrate, a porphyrin analog, purpurin-18 (Pp-18), which is not a substrate for P-gp or MRP1. The ability of inhibitors to block efflux activity of ABCG2 was assessed using Pp-18. Inhibitors also demonstrated similar effects on human and mouse ABCG2. Chrysin, benzoflavone, and cyclosporin A inhibited Pp-18 efflux in both human and mouse ABCG2. The similarity of the substrate and inhibitor specificity of human and mouse ABCG2 supports interpretation of mouse models in understanding the clinical, pharmacological and physiological roles of ABCG2.

Introduction

ABCG2 (also known as breast cancer resistance protein; BCRP) is an ATP-binding cassette (ABC) transporter localized to the plasma membrane that actively pumps a wide variety of molecules out of cells. ABCG2 was first identified in multidrug-resistant cancer cell lines (Polgar et al., 2008), but it also plays a protective role at the maternal-fetal, blood-testis and blood-brain barriers by preventing the entry of small molecules (Kannan et al., 2009; Robey et al., 2009). It facilitates absorption in the liver and limits absorption from the small intestine, and it is expressed in the mammary glands where it is responsible for active secretion of substrates into milk (Jonker et al., 2005). ABCG2 function is responsible for the 'side-population' phenomenon observed in flow cytometry due to Hoechst 33342 efflux by hematopoietic cells with stem-cell-like characteristics (Natarajan et al., 2012). When Abcg2 is absent in transgenic mice, the primary phenotype is photosensitivity, with phototoxic lesions due to the accumulation of endogenous porphyrin metabolites that would otherwise be excreted (Jonker et al., 2002), and it was recently shown that Abcg2 mediates the transport of sulfate conjugates of phytoestrogens (Van de Wetering and Sapthu, 2012). Polymorphic forms of ABCG2 are associated with gout because of decreased excretion of uric acid in the proximal tubule of the kidney (Woodward et al., 2009). It was recently recognized that healthy individuals of the Jr(a)- blood type carry two null alleles of ABCG2 despite the important physiologic role understood for ABCG2 (Saison et al., 2012; Zelinski et al., 2012). The functional consequences of ABCG2 loss are still unknown, but are not associated with obvious disease. In light of the roles of ABCG2 in drug resistance and normal physiology, further research on models aimed at understanding ABCG2 function is warranted.

Cell lines expressing human ABCG2 are commonly used to study its function as an efflux pump or to screen for novel inhibitors (Deeken et al., 2009). Fluorescent substrates have proven to be useful tools for measuring transporter function, and *in vitro* studies using these substrates are sometimes reported alongside pharmacokinetic assessments in *Abcg2* knockout mice to study ABCG2 function *in vivo* (Kannan et al., 2010; Hall and Pike, 2011; Mairinger et al., 2011). Abcg2-deficient mice have also been instrumental in elucidating the normal physiologic roles of ABCG2, such as its role in preventing oral drug absorption or brain penetration of substrates (Vlaming et al., 2009). The mouse ortholog of ABCG2 has 81% protein sequence homology with human ABCG2 (Allen et al., 1999) and a single amino acid mutation can alter the substrate and antagonist specificity in both species (Robey et al., 2003), leading to the assumption that substrate and inhibitor profiles of human and murine ABCG2 are directly comparable. However, in the case of P-glycoprotein (P-gp, ABCB1), significantly different substrate and inhibitor specificities have been observed between species (Pike, 2009; Syvanen et al., 2009). Baltes *et al.* (2007) demonstrated that phenytoin and levetiracetam were transported by mouse but not human Pg-p (Baltes et al., 2007). Differences in inhibitor efficacy have also been suggested for human and mouse ABCG2 (Zhang et al., 2005). This suggests caution when extrapolating data from mouse models to humans. The comparative specificity of substrates and inhibitors in human versus mouse ABCG2 is still unclear and warrants further investigation.

In this study, the abilities of cell lines expressing human or mouse ABCG2 to efflux fluorescent substrates were compared using flow cytometry. The genomic sequence and protein expression of ABCG2 was assessed in the cell lines. A new fluorescent porphyrin substrate, purpurin-18 (Pp-18) was identified, and demonstrated to be transported by mouse and human

ABCG2, but not P-gp or MRP1. The ability of inhibitors to block efflux activity of human and mouse ABCG2 was assessed using Pp-18 as a substrate.

Materials and Methods

Chemicals. Pheophorbide a, pyropheophorbide a methyl ester, chlorin e6, and purpurin-18 were obtained from Frontier Scientific (Logan, UT). Flavopiridol was obtained from the National Cancer Institute Anticancer Drug Screen (Bethesda, MD). BODIPY-prazosin, a conjugate of the ABCG2 substrate with a boron-dipyrromethene fluorescent dye, was obtained from Molecular Probes (Eugene, OR, USA). Ko143 was purchased from Tocris Bioscience (Minneapolis, MN). Nilotinib (AMN107) was purchased from Novartis (Basel, Switzerland). NSC73306 was synthesized as previously reported (Hall et al., 2011). Benzoflavone was purchased from Indofine (Hillsborough, NJ). Vismodegib was purchased from Selleck Chemicals (Houston, TX). Elacridar (GF120918) and tariquidar (XR9576) were purchased from MedKoo Biosciences (Chapel Hill, NC). DCPQ was provided by Dr. Victor W. Pike, National Institutes of Mental Health (Bethesda, MD). Daunorubicin (daunomycin), rhodamine 123, novobiocin (albamycin) and all other chemicals were purchased from Sigma-Aldrich (St. Louis, MO) unless stated otherwise.

Cell Lines. The parental (control) and resistant (ABC transporter-expressing) cell lines used in this study were (drug selection shown in parentheses): 3T3 and its Abcg2-expressing subline 3T3 MX15 (15 nM mitoxantrone), and its P-gp-expressing subline 3T3 C3M (1 μ g/mL colchicine) (Hall et al., 2011), the mouse fibroblast line Ltk- and its Abcg2-expressing subline Ltk- HoeR415 (1 μM Hoechst 33342) (Smith et al., 2009), the mouse fibroblast MEF3.8, and its Abcg2-expressing subline MEF3.8 M32 (32 nM mitoxantrone) (Allen et al., 1999), the human

large cell lung cancer cell line H460 and its ABCG2-expressing subline H460 MX20 (20 nM mitoxantrone) (Robey et al., 2004), the human breast cancer cell line MCF-7, its ABCG2-expressing subline MCF-7 FLV500 (500 nM flavopiridol) (Robey et al., 2001b) and its MRP1-expressing subline MCF-7 VP-16 (16 nM etoposide) (Schneider et al., 1994); the human adenocarcinoma cell line KB-3-1 and its P-gp-expressing subline KB-8-5-11 (250 nM colchicine) (Shen et al., 1986). All cells were grown at 37°C in 5% CO_2 and were maintained either in RPMI or DMEM medium supplemented with 10% fetal bovine serum, penicillin, and streptomycin. Medium was removed and cells were grown in the same medium in the absence of drug selection 5 to 30 days before assay.

The mouse fibroblast 3T3 MX15 subline was selected by exposing NIH 3T3 cells to increasing concentrations of mitoxantrone (1nM – 15 nM). The Ltk- mouse cell line was developed from a subline of the BrdU-resistant strain of the L-M mouse line (Kit et al., 1963). The Ltk- drug-selected subline (Ltk- HoeR415) has been shown to have increased Abcg2 expression and function (Smith et al., 1988; Smith et al., 2009). The Ltk- and Ltk- HoeR415 were provided by Paul J. Smith (Cardiff University). The MEF3.8 cell line was derived from Mdr1a/b$^{-/-}$ Mrp1$^{-/-}$ mice and the MEF3.8 M32 subline were provided by Alfred H. Schinkel (Netherlands Cancer Institute). The human ABCG2-expressing sublines used (H460 MX20 and MCF7 FLV500) have been previously characterized (Robey et al., 2001b; Robey et al., 2004).

Simple Western. An automated capillary-based Simple Western system (Simon, ProteinSimple) was used to quantify the levels of ABCG2 and P-gp. Automation allows more accurate and reproducible assessment of protein levels compared to traditional Western blots

(Nguyen et al., 2011). Samples were analyzed as previously described unless stated otherwise (Kohn et al., 2012). In brief, samples containing the same amount of protein, 57 ng (mouse) or 20 ng (human) for ABCG2 analysis and 20 ng (human and mouse) for P-gp analysis, were used. The target proteins were immunoprobed for ABCG2 using monoclonal BXP-53 antibody (Abcam) and for P-gp expression using monoclonal C219 antibody (Fujirebio Diagnostics, Inc.) and for tubulin using anti- α-tubulin (Cell Signaling Technologies). For quantitative data analysis, the ABCG2 and P-gp signals were normalized against α-tubulin as a loading control.

Cytotoxicity Assay. Cytotoxicity was measured with a luminescent cell viability assay (CellTiter Glo by Promega). Stock solutions of cytotoxic drugs were prepared in RPMI medium. Cultured cells were seeded 3,000 cells/well and incubated in serial dilutions of the compound for 72 h. before assaying cell growth, as described by (Brimacombe et al., 2009). Cytotoxicity (IC_{50}) was defined as the drug concentration that reduced cell viability to 50% of the untreated control and was calculated from three independent experiments.

Flow Cytometry. For each condition, 10^6 cells were suspended in IMDM supplemented with 5% fetal bovine serum. After addition of the fluorescent substrate with or without the inhibitor of interest, cells were incubated in the dark for 30 min at 37 °C. Concentrations used were based on values reported in the literature (as cited elsewhere). In some instances, higher concentrations were employed to ensure inhibitory activity was easily resolved by flow cytometry. They were then washed and allowed to efflux in substrate-free media for 30 min under the same conditions, then centrifuged, resuspended in ice-cold phosphate-buffered saline, and kept on ice until analysis (within 1 h.). Cells were gated for forward versus side scatter and

the geometric mean of fluorescence intensity (cellular uptake of fluorescent substrate) was recorded for a total of 20,000 cells using a LSR II flow cytometer (BD Biosciences, San Jose, CA) under the excitation emission wavelengths listed in Table 1. Fluorescence-activated cell sorting data were analyzed using FlowJo software (Tree Star, Inc., Ashland, OR).

Statistical Analysis. Data are expressed as mean ± S.D. from three observations for fluorescence accumulation assays and cytotoxicity assays. After the data were tested for homogeneity of variance, statistical significance was evaluated by the Student's t test (unpaired, two-tailed, α = 0.05) and by a two-way ANOVA followed by the Bonferroni post-t test (α = 0.05).

DMD Fast Forward. Published on July 18, 2013 as DOI: 10.1124/dmd.113.053140
This article has not been copyedited and formatted. The final version may differ from this version.

Results

Generation of Mitoxantrone-Resistant Mouse Fibroblast Line Over-Expressing ABCG2.

Exposure to mitoxantrone in incremental doses can select for expression of ABCG2 (Robey et al., 2001a). Here, NIH 3T3 fibroblasts were passaged with increasing mitoxantrone concentrations (1nM – 15 nM) over a period of three months. Quantitative immunodetection of protein from NIH 3T3 and its selected mitoxantrone-resistant subline 3T3 MX15 demonstrated increased levels of ABCG2 (Fig. 1). While resistance to mitoxantrone may also result from increased expression of P-gp, this was not significantly overexpressed in 3T3 MX15 cells (Supplemental Fig. 1). To confirm that the resistance phenotype was mediated by Abcg2, we performed cytotoxicity assays with mitoxantrone in the presence or absence of the ABCG2 inhibitor, Ko143 (5 μM). The 3T3 MX15 cells (IC_{50} = 134.6 ± 28.2 μM) were 33-fold more resistant to mitoxantrone relative to the parental cells (IC_{50} = 4.0 ± 2.0 μM). Resistance decreased to 5-fold in the presence of Ko143 (3T3 IC_{50} 1.7 ± 0.2 μM and MX15 IC_{50} 10.0 ± 8.0 μM). Both cell lines were sensitized by Ko143 to mitoxantrone, confirming that 3T3 cells express low levels of Abcg2, as previously reported (Allen et al., 2000), and seen here by the electropherogram (Fig. 1). Functional Abcg2 was determined by the ability to efflux fluorescent ABCG2 substrates and analyzed by flow cytometery (Table 1). For example, 3T3 MX15 cells demonstrated a significantly lower accumulation of ABCG2 substrates than 3T3 cells (see below Table 1 and Supplemental Fig. 2), which increased in the presence of Ko143.

Human and Mouse ABCG2 Demonstrated an Overlap in Efflux of Fluorescent Substrates.

In this study, we examined independent drug-selected mouse and human ABCG2-expressing sub-lines with their respective parental lines (two pairs from each species, Fig. 1,

Supplemental Fig. 1 and Fig 3). A third mouse fibroblast cell line was used when a difference was observed (discussed below). Mutations at amino-acid 482 in human and mouse ABCG2 can affect substrate and antagonist specificity (Allen et al., 2002a; Robey et al., 2003). This region has been suggested as a mutation hotspot acquired in highly drug-resistant cells. Therefore the mouse cell lines 3T3, 3T3 MX15, Ltk- and Ltk- HoeR415 were sequenced to check for this mutation. Sequencing data showed homozygous wild-type sequence (arginine codon AGG) in all cell lines, with no trace of secondary mutant DNA signatures (Supplemental Fig. 4). In the other cell lines used in this study, this region has been previously characterized as wild-type (Allen et al., 2002a; Honjo et al., 2002; Volk et al., 2002).

To evaluate fluorescent substrates of human and mouse ABCG2, we conducted efflux studies using flow cytometry. Cells were incubated with fluorescent substrates identified from the literature (Table 1) with or without inhibitor (10 μM Ko143), washed, and then allowed to efflux in substrate-free media under the same conditions. The compounds studied were mitoxantrone, Hoechst 33342, BODIPY-prazosin, rhodamine 123, daunorubicin, pheophorbide a, pyropheophorbide a methyl ester (MPPa) and chlorin e6 (Polgar et al., 2008). Daunorubicin and rhodamine 123 were assessed because they are transported by the R482 mutant but not wild-type ABCG2 (Robey et al., 2003). Cell fluorescence was normalized to the value derived in ABCG2-expressing cells in the presence of Ko143 (i.e., cells with fully inhibited ABCG2) and the percentage (%) difference with and without the inhibitor is displayed for ABCG2-expressing cells in Table 1. Accumulation levels for both parental and ABCG2 cells for each compound are shown in Supplemental Fig. 2. Mitoxantrone, Hoechst 33342, BODIPY-prazosin, pheophorbide a, MPPa, and chlorin e6 demonstrated significant efflux in human and mouse ABCG2-

expressing cells when compared to parental cells (Supplemental Fig. 2) and the accumulation of substrates increased when co-incubated with Ko143 (10 μM) (Table 1). Daunorubicin accumulation did not significantly differ in the human and mouse ABCG2-expressing cells when inhibited, or compared to parental cells. The average percentage efflux of most substrates by human and mouse ABCG2 did not demonstrate a significant difference (Fig. 2).

Rhodamine 123 efflux was observed in mouse (not human) Abcg2-expressing sublines, (Supplemental Fig. 2 and 5) but this was due to P-gp efflux. Accumulation of rhodamine 123 increased ~2-3 fold in the presence of the P-gp inhibitors PSC833 and DCPQ and ~1.5 fold in the presence of Ko143 at high concentrations (Supplemental Fig. 6). Additionally, rhodamine 123 efflux was not observed in a mouse fibroblast cell line derived from a P-gp knockout mouse (MEF3.2) and its Abcg2-expressing subline (MEF 3.2 M32) (Supplemental Figure 5b). The accumulation of mitoxantrone, daunorubicin, BODIPY-prazosin, and Hoechst 33342 was tested with and without a specific P-gp inhibitor (1 μM DCPQ) since they are weak substrates of P-gp. Mitoxantrone and daunorubicin accumulation did not significantly increase in the presence of a specific P-gp inhibitor. However, BODIPY-prazosin and Hoechst 33342 accumulation did increase in the presence of a specific P-gp inhibitor (Supplemental Fig. 7), but the difference was smaller than that due to Abcg2 efflux (Supplemental Fig. 2). Therefore, our data suggest that the low baseline P-gp in the mouse cell lines is not a major participant in the transport of mitoxantrone, Hoechst 33342 and BODIPY-prazosin.

Purpurin-18, a Porphyrin Derivative, is a Specific Substrate of Human and Mouse ABCG2. In addition to other known porphyrin ABCG2 substrates that are used for

photodynamic therapy (Robey et al., 2004; Robey et al., 2005), we investigated purpurin-18 (Pp-18) (structure shown in Fig. 3A) as a potential new porphyrin substrate of ABCG2 by efflux studies with ABCG2-overexpressing sublines (Fig. 3B and Supplemental Fig. 2). Efflux of Pp-18 by parental cells (top row, Fig. 3B) was compared with efflux of Pp-18 from ABCG2-expressing cells (bottom row, Fig. 3B). In the parental cells, a small but detectable amount of inhibitable Pp-18 efflux was observed when these cells were incubated in Pp-18 without (grey line) or with (black line) Ko143. To evaluate the ABCG2 specificity of Pp-18 among ABC transporters, we conducted efflux studies on sublines overexpressing human P-gp (KB-8-5-11) and MRP1 (VP16), and mouse P-gp (C3M) compared with their parental lines (KB-3-1, MCF7 and 3T3, respectively). Cells were incubated with Pp-18 with or without their respective transport inhibitor (20 μM verapamil for P-gp; 100 μM indomethacin for MRP1). No significant differences were observed in the accumulation of Pp-18 between parental and transporter-expressing lines for human P-gp or MRP1 (Fig. 3C), and mouse P-gp (Fig. 3D), though a small non-specific effect was evident in all cells. Pp-18 is a therefore a specific substrate for human and mouse ABCG2, and can be used to test the effect of inhibitors on ABCG2 efflux.

Inhibitors Demonstrated a Similar Effect on Human and Mouse ABCG2-Mediated Efflux of Pp-18. We next examined the inhibition of Pp-18 efflux to assess reported inhibitors of ABCG2-mediated drug resistance (Table 2, Figure 2B and Supplemental Fig. 8). Small molecules reported as inhibitors or competitive substrates of ABCG2 were assessed: flavopiridol, elacridar, tariquidar, nilotinib, quercetin, 17-β-estradiol, novobiocin, cyclosporin A (Polgar et al., 2008), NSC73306 (Wu et al., 2007), chrysin (Zhang et al., 2005), benzoflavone (Zhang et al., 2005), and vismodegib (Zhang et al., 2009). Sulfasalazine is an ABCG2 substrate (van der

Heijden et al., 2004) and we tested if sulfasalazine can act as a competitive inhibitor (Ambudkar et al., 1999). Ko143 (Allen et al., 2002b) and fumitremorgin C (FTC) (Rabindran et al., 1998) were included as positive controls. The fold value is defined as the accumulation of Pp-18 in the presence of an inhibitor divided by the accumulation of Pp-18 in the absence of an inhibitor. Elacridar, tariquidar, nilotinib, quercetin, NSC73306, flavopiridol, chrysin, benzoflavone, 17- β -Estradiol, novobiocin, and vismodegib all demonstrated a significant increase in Pp-18 accumulation in both human and mouse ABCG2-expressing cell lines (Table 2 and Supplemental Fig. 8). A significant difference between the average fold values of mouse and human ABCG2 was not observed (Figure 2B). Sulfazalazine did not inhibit either human or mouse ABCG2 efflux of Pp-18. Quercetin, sulfasalazine, NSC73306, chrysin, 17- β -estradiol, novobiocin, and vismodegib were examined at lower concentrations (10 μM), and exhibited the same relative inhibition profile against all four cell lines (Supplemental Fig. 9).

Given conflicting reports that cyclosporin A inhibits ABCG2 function (Ejendal and Hrycyna, 2005; Gupta et al., 2006), we tested its ability to inhibit the efflux of Pp-18 in a dose dependent manner (Fig. 4). We observed a dose-dependent increase in accumulation of Pp-18 when cyclosporin A (1, 5, 10, 25, 50 μM) was added. Incubation with cyclosporin A at 50 μM demonstrated a similar inhibition profile to Ko143 in the Ltk- HoeR415 subline.

Discussion

ABCG2 has a well-established role in limiting the oral bioavailability of substrates as well as limiting brain penetration and facilitating renal excretion of compounds. Abcg2-deficient mouse models have been extensively used to confirm these roles, as well as to test the ability of ABCG2 inhibitors to limit brain penetration or increase oral absorption of drugs. Despite this, few studies have been performed to assess the overlapping substrate specificity of human and murine ABCG2. To compare mouse and human ABCG2 function, we used human and mouse ABCG2-expressing sublines (and their parental lines) that were independently drug selected. To this end, we generated a mouse Abcg2-expressing subline (3T3 MX15) by long-term selection in mitoxantrone. We found that the ABCG2 substrates examined were similarly transported by human and mouse ABCG2. This suggests that human ABCG2 transporter substrate interactions may be extrapolated to mouse Abcg2 function for the tested substrates. Additionally, the fluorescent substrates examined here can be used to confirm that inhibitors of human ABCG2 can be used to inhibit murine Abcg2 when used in mouse models.

We evaluated the inhibition of mouse and human ABCG2 using Purpurin-18 as the substrate. Known ABCG2 inhibitors demonstrated a similar pattern of inhibiting Pp-18 efflux in human and mouse ABCG2-expressing cells. Ko143 and FTC are considered to be 'general' inhibitors of ABCG2 in that they inhibit ATPase activity of ABCG2. Alternatively, the remaining inhibitors have been demonstrated to be substrates of ABCG2, and as such act as competitive inhibitors. It has previously been reported that chrysin and benzoflavone can inhibit human but not mouse Abcg2 (Zhang et al., 2005). Zhang *et al.* (2005) observed inhibition of topotecan efflux in human ABCG2-expressing cells. However, these inhibitors did not alter

mouse topotecan pharmacokinetics *in vivo* and did not significantly inhibit mouse Abcg2-expressing cells. This was attributed to species differences of ABCG2. We observed a significant fold-increase in Pp-18 accumulation (comparable to inhibition by FTC or Ko143) in mouse and human ABCG2-expressing cell lines when adding the same concentrations of chrysin and benzoflavone used by Zhang *et al*. Due to the existence of multiple binding sites on ABCG2 (Giri et al., 2009), there may be different transporter mediated interactions, and competitive substrates may not inhibit the efflux of all transport substrates. As such, caution should be taken that an inhibitor of ABCG2 is dependent on the substrates tested.

Flavoperidol and nilotininb are ABCG2 substrates, and can inhibit ABC transporter function at high concentrations as competitive substrates. Sulfasalazine (a known ABCG2 substrate) did not inhibit human or mouse ABCG2, and we also did not observe an increased uptake of other fluorescent substrates by sulfasalazine (data not shown). Some inhibition was noted in the HoeR415 Abcg2-expressing cell line that expressed the least ABCG2 of the cell lines used at 100 μM. The weak effect may to the carboxylic acid of sulfasalazine rendering the molecule negative at physiologic pH, reducing its cell membrane permeability.

There is a longstanding question on the interaction of cyclosporin A with ABCG2 due to conflicting reports. In the presence of cyclosporin A (~5-10 μM) Ejendal *et al.* (2005) did not observe displacement of a photoaffinity analog of prazosin, increased fluorescence accumulation of mitoxantrone or an effect on prazosin ATPase activity by cyclosporin A and concluded it does not inhibit ABCG2 (Ejendal and Hrycyna, 2005) . However, Gupta *et al.* reported that cyclosporin A (~1-10 μM) significantly inhibited ABCG2 efflux of BODIPY-prazosin,

mitoxantrone, and pheophorbide A and concluded that cyclosporin A can inhibit ABCG2 (Gupta et al., 2006). Our studies indicated that cyclosporin A inhibited human and mouse ABCG2 efflux of Pp-18 in a dose dependent manner that correlated with the amount of ABCG2 expressed at the cell membrane. The addition of cyclosporin A produced the highest fold-increase in the cells with the lowest expression of ABCG2 (Ltk- HoeR415) and this interaction was masked in the cells with higher ABCG2 expression when lower concentrations of cyclosporin A were used (~1-5 μM) (Fig. 4) Cyclosporin A (5 μM) also increased the accumulation of BODIPY-prazosin in H460 MX20 (Supplemental Fig. 10), confirming the ability of cyclosporin A to act as an ABCG2 inhibitor.

We identified a new specific human and mouse ABCG2 porphyrin substrate, purpurin-18 (Pp-18). Porphyrins have proven useful in fluorescence-guided resections and treatment of cancer (Sun et al., 2013) and are known ABCG2 substrates (Jonker et al., 2002). Pp-18 is a natural red-emitting fluorescent product of chlorophyll and is a photosensitizer with cell-targeting utility (via covalent attachment to antibodies due to an anhydride group)(Hoober et al., 1988) (Sharma et al., 2006). Far-red emitting markers are more useful than those emitting blue-green light due to low background autofluorescence and also provide maximal tissue penetration (Edward, 2012). The expression of the ABCG2 transporter plays a significant role in the efflux of porphyrins from cells, as seen with Pp-18 efflux by ABCG2. Understanding the role of ABCG2 and its inhibition in order to increase the accumulation of porphyrins to improve therapeutic efficiency has great clinical implications for malignant gliomas (Sun et al., 2013). Despite new treatment modalities, patients with aggressive glioblastoma have a median survival rate of less than 15 months, and multiple resections are often necessary to prolong survival

(Chaichana et al., 2013). One reason for this poor prognosis may be due to the function of ABCG2, which enables resistance to treatment as well as escape from fluorescence-guided resections. Additionally, ABCG2 is commonly found in the “side-population” of cells implicated in gliomagenesis (Bleau et al., 2009) and may play a role in the recurrence of glioblastoma. Given that Pp-18 is extruded by mouse and human ABCG2 and it is not a substrate for human P-gp or MRP1 or mouse P-gp (Fig. 3) it may be useful for pre-clinical mouse models to study ABCG2 function.

The ABCG2 protein plays an important role in a variety of physiological and pathological functions. It can protect the body from xenobiotics but it also confers multi-drug resistance in cancer cells. ABCG2−/− (Jr(a−)) individuals exist and the functional consequence on normal physiology drug pharmacodynamics is still not known. Therefore, the substrate and inhibitor overlap of mouse and human ABCG2 substantiates the use of mouse models with potential clinical implications.

Acknowledgments. Joshua Bakhsheshian is an NIH Medical Research Scholar. We thank Karen M. Wolcott for flow cytometry assistance, Dominic Esposito and Vanessa Wall for gene sequencing assistance, and George Leiman for editorial assistance.

Authorship Contributions

Participated in research design: Bakhsheshian, Hall, Robey, Bates, Gottesman

Conducted Experiments: Bakhsheshian, Herrmann, Chen

Performed data analysis: Bakhsheshian, Hall, Herrmann, Chen, Robey

Wrote or contributed to the writing of the manuscript: Bakhsheshian, Hall, Robey, Bates, Gottesman

References

Allen JD, Brinkhuis RF, van Deemter L, Wijnholds J, and Schinkel AH (2000) Extensive contribution of the multidrug transporters P-glycoprotein and Mrp1 to basal drug resistance. *Cancer Res* **60:**5761-5766.

Allen JD, Brinkhuis RF, Wijnholds J, and Schinkel AH (1999) The mouse Bcrp1/Mxr/Abcp gene: amplification and overexpression in cell lines selected for resistance to topotecan, mitoxantrone, or doxorubicin. *Cancer Res* **59:**4237-4241.

Allen JD, Jackson SC, and Schinkel AH (2002a) A mutation hot spot in the Bcrp1 (Abcg2) multidrug transporter in mouse cell lines selected for Doxorubicin resistance. *Cancer Res* **62:**2294-2299.

Allen JD, van Loevezijn A, Lakhai JM, van der Valk M, van Tellingen O, Reid G, Schellens JH, Koomen GJ, and Schinkel AH (2002b) Potent and specific inhibition of the breast cancer resistance protein multidrug transporter in vitro and in mouse intestine by a novel analogue of fumitremorgin C. *Mol Cancer Ther* **1:**417-425.

Ambudkar SV, Dey S, Hrycyna CA, Ramachandra M, Pastan I, and Gottesman MM (1999) Biochemical, cellular, and pharmacological aspects of the multidrug transporter. *Ann Rev Pharmacol Toxicol* **39:**361-398.

Baltes S, Gastens AM, Fedrowitz M, Potschka H, Kaever V, and Loscher W (2007) Differences in the transport of the antiepileptic drugs phenytoin, levetiracetam and carbamazepine by human and mouse P-glycoprotein. *Neuropharmacol* **52:**333-346.

Bleau AM, Huse JT, and Holland EC (2009) The ABCG2 resistance network of glioblastoma. *Cell Cycle* **8:**2936-2944.

Brimacombe KR, Hall MD, Auld DS, Inglese J, Austin CP, Gottesman MM, and Fung KL (2009) A dual-fluorescence high-throughput cell line system for probing multidrug resistance. *Assay Drug Dev Technol* **7:**233-249.

Chaichana KL, Zadnik P, Weingart JD, Olivi A, Gallia GL, Blakeley J, Lim M, Brem H, and Quinones-Hinojosa A (2013) Multiple resections for patients with glioblastoma: prolonging survival. *J Neurosurgery* **118:**812-820.

Deeken JF, Robey RW, Shukla S, Steadman K, Chakraborty AR, Poonkuzhali B, Schuetz EG, Holbeck S, Ambudkar SV, and Bates SE (2009) Identification of compounds that correlate with ABCG2 transporter function in the National Cancer Institute Anticancer Drug Screen. *Mol Pharmacol* **76:**946-956.

Edward R (2012) Red/far-red fluorescing DNA-specific anthraquinones for nucl:cyto segmentation and viability reporting in cell-based assays. *Methods in enzymology* **505:**23-45.

Ejendal KF and Hrycyna CA (2005) Differential sensitivities of the human ATP-binding cassette transporters ABCG2 and P-glycoprotein to cyclosporin A. *Mol Pharmacol* **67:**902-911.

Giri N, Agarwal S, Shaik N, Pan G, Chen Y, and Elmquist WF (2009) Substrate-dependent breast cancer resistance protein (Bcrp1/Abcg2)-mediated interactions: consideration of multiple binding sites in in vitro assay design. *Drug Metab Dispos* **37:**560-570.

Gupta A, Dai Y, Vethanayagam RR, Hebert MF, Thummel KE, Unadkat JD, Ross DD, and Mao Q (2006) Cyclosporin A, tacrolimus and sirolimus are potent inhibitors of the human breast cancer resistance protein (ABCG2) and reverse resistance to mitoxantrone and topotecan. *Cancer Chemother Pharmacol* **58:**374-383.

Hall MD, Brimacombe KR, Varonka MS, Pluchino KM, Monda JK, Li J, Walsh MJ, Boxer MB, Warren TH, Fales HM, and Gottesman MM (2011) Synthesis and structure-activity evaluation of isatin-beta-thiosemicarbazones with improved selective activity toward multidrug-resistant cells expressing P-glycoprotein. *J Med Chem* **54:**5878-5889.

Hall MD and Pike VW (2011) Avoiding barriers to PET radioligand development: cellular assays of brain efflux transporters. *J Nuclear Med* **52:**338-340.

Honjo Y, Morisaki K, Huff LM, Robey RW, Hung J, Dean M, and Bates SE (2002) Single-nucleotide polymorphism (SNP) analysis in the ABC half-transporter ABCG2 (MXR/BCRP/ABCP1). *Cancer Biol Ther* **1:**696-702.

Hoober JK, Sery TW, and Yamamoto N (1988) Photodynamic sensitizers from chlorophyll: purpurin-18 and chlorin p6. *Photochem Photobiol* **48:**579-582.

Jonker JW, Buitelaar M, Wagenaar E, Van Der Valk MA, Scheffer GL, Scheper RJ, Plosch T, Kuipers F, Elferink RP, Rosing H, Beijnen JH, and Schinkel AH (2002) The breast cancer resistance protein protects against a major chlorophyll-derived dietary phototoxin and protoporphyria. *Proc Natl Acad Sci U S A* **99:**15649-15654.

Jonker JW, Merino G, Musters S, van Herwaarden AE, Bolscher E, Wagenaar E, Mesman E, Dale TC, and Schinkel AH (2005) The breast cancer resistance protein BCRP (ABCG2) concentrates drugs and carcinogenic xenotoxins into milk. *Nat Med* **11:**127-129.

Kannan P, Brimacombe KR, Zoghbi SS, Liow JS, Morse C, Taku AK, Pike VW, Halldin C, Innis RB, Gottesman MM, and Hall MD (2010) N-desmethyl-loperamide is selective for P-glycoprotein among three ATP-binding cassette transporters at the blood-brain barrier. *Drug Metab Dispos* **38:**917-922.

Kannan P, John C, Zoghbi SS, Halldin C, Gottesman MM, Innis RB, and Hall MD (2009) Imaging the function of P-glycoprotein with radiotracers: pharmacokinetics and in vivo applications. *Clin Pharmacol Ther* **86:**368-377.

Kit S, Dubbs DR, Piekarski LJ, and Hsu TC (1963) Deletion of Thymidine Kinase Activity from L Cells Resistant to Bromodeoxyuridine. *Exp Cell Res* **31:**297-312.

Kohn EA, Yang YA, Du Z, Nagano Y, Van Schyndle CM, Herrmann MA, Heldman M, Chen JQ, Stuelten CH, Flanders KC, and Wakefield LM (2012) Biological responses to TGF-beta in the mammary epithelium show a complex dependency on Smad3 gene dosage with important implications for tumor progression. *Mol Cancer Res* **10:**1389-1399.

Mairinger S, Erker T, Muller M, and Langer O (2011) PET and SPECT radiotracers to assess function and expression of ABC transporters in vivo. *Curr Drug Metab* **12:**774-792.

Natarajan K, Xie Y, Baer MR, and Ross DD (2012) Role of breast cancer resistance protein (BCRP/ABCG2) in cancer drug resistance. *Biochem Pharmacol* **83:**1084-1103.

Nguyen U, Squaglia N, Boge A, and Fung PA (2011) The Simple Western [trade]: a gel-free, blot-free, hands-free Western blotting reinvention. *Nat Methods* **8**.

Pike VW (2009) PET radiotracers: crossing the blood-brain barrier and surviving metabolism. *Trends Pharmacol Sci* **30:**431-440.

Polgar O, Robey RW, and Bates SE (2008) ABCG2: structure, function and role in drug response. *Expert Opin Drug Metab Toxicol* **4:**1-15.

Rabindran SK, He H, Singh M, Brown E, Collins KI, Annable T, and Greenberger LM (1998) Reversal of a novel multidrug resistance mechanism in human colon carcinoma cells by fumitremorgin C. *Cancer Res* **58:**5850-5858.

Robey RW, Honjo Y, Morisaki K, Nadjem TA, Runge S, Risbood M, Poruchynsky MS, and Bates SE (2003) Mutations at amino-acid 482 in the ABCG2 gene affect substrate and antagonist specificity. *Br J Cancer* **89:**1971-1978.

Robey RW, Honjo Y, van de Laar A, Miyake K, Regis JT, Litman T, and Bates SE (2001a) A functional assay for detection of the mitoxantrone resistance protein, MXR (ABCG2). *Biochim Biophys Acta* **1512:**171-182.

Robey RW, Medina-Perez WY, Nishiyama K, Lahusen T, Miyake K, Litman T, Senderowicz AM, Ross DD, and Bates SE (2001b) Overexpression of the ATP-binding cassette half-transporter, ABCG2 (Mxr/BCrp/ABCP1), in flavopiridol-resistant human breast cancer cells. *Clin Cancer Res* **7:**145-152.

Robey RW, Steadman K, Polgar O, and Bates SE (2005) ABCG2-mediated transport of photosensitizers: potential impact on photodynamic therapy. *Cancer Biol Ther* **4:**187-194.

Robey RW, Steadman K, Polgar O, Morisaki K, Blayney M, Mistry P, and Bates SE (2004) Pheophorbide a is a specific probe for ABCG2 function and inhibition. *Cancer Res* **64:**1242-1246.

Robey RW, To KK, Polgar O, Dohse M, Fetsch P, Dean M, and Bates SE (2009) ABCG2: a perspective. *Adv Drug Delivery Rev* **61:**3-13.

Saison C, Helias V, Ballif BA, Peyrard T, Puy H, Miyazaki T, Perrot S, Vayssier-Taussat M, Waldner M, Le Pennec PY, Cartron JP, and Arnaud L (2012) Null alleles of ABCG2 encoding the breast cancer resistance protein define the new blood group system Junior. *Nat Genet* **44:**174-177.

Schneider E, Horton JK, Yang CH, Nakagawa M, and Cowan KH (1994) Multidrug resistance-associated protein gene overexpression and reduced drug sensitivity of topoisomerase II in a human breast carcinoma MCF7 cell line selected for etoposide resistance. *Cancer Res* **54:**152-158.

Sharma S, Dube A, Bose B, and Gupta PK (2006) Pharmacokinetics and phototoxicity of purpurin-18 in human colon carcinoma cells using liposomes as delivery vehicles. *Cancer Chemother Pharmacol* **57:**500-506.

Shen DW, Cardarelli C, Hwang J, Cornwell M, Richert N, Ishii S, Pastan I, and Gottesman MM (1986) Multiple drug-resistant human KB carcinoma cells independently selected for high-level resistance to colchicine, adriamycin, or vinblastine show changes in expression of specific proteins. *J Biol Chem* **261:**7762-7770.

Smith PJ, Furon E, Wiltshire M, Campbell L, Feeney GP, Snyder RD, and Errington RJ (2009) ABCG2-associated resistance to Hoechst 33342 and topotecan in a murine cell model with constitutive expression of side population characteristics. *Cytometry Part A* **75:**924-933.

Smith PJ, Lacy M, Debenham PG, and Watson JV (1988) A mammalian cell mutant with enhanced capacity to dissociate a bis-benzimidazole dye-DNA complex. *Carcinogenesis* **9:**485-490.

Sun W, Kajimoto Y, Inoue H, Miyatake S, Ishikawa T, and Kuroiwa T (2013) Gefitinib enhances the efficacy of photodynamic therapy using 5-aminolevulinic acid in malignant brain tumor cells. *Photodiagnosis Photodynamic Ther* **10:**42-50.

Syvanen S, Lindhe O, Palner M, Kornum BR, Rahman O, Langstrom B, Knudsen GM, and Hammarlund-Udenaes M (2009) Species differences in blood-brain barrier transport of

three positron emission tomography radioligands with emphasis on P-glycoprotein transport. *Drug Metab Dispos* **37:**635-643.

van der Heijden J, de Jong MC, Dijkmans BA, Lems WF, Oerlemans R, Kathmann I, Scheffer GL, Scheper RJ, Assaraf YG, and Jansen G (2004) Acquired resistance of human T cells to sulfasalazine: stability of the resistant phenotype and sensitivity to non-related DMARDs. *Ann Rheum Dis* **63:**131-137.

van de Wetering K, Sapthu S (2012) ABCG2 functions as a general phytoestrogen sulfate transporter in vivo. *FASEB J*. **26**:4014-4024.

Vlaming ML, Lagas JS, and Schinkel AH (2009) Physiological and pharmacological roles of ABCG2 (BCRP): recent findings in Abcg2 knockout mice. *Adv Drug Delivery Rev* **61:**14-25.

Volk EL, Farley KM, Wu Y, Li F, Robey RW, and Schneider E (2002) Overexpression of wild-type breast cancer resistance protein mediates methotrexate resistance. *Cancer Res* **62:**5035-5040.

Woodward OM, Kottgen A, Coresh J, Boerwinkle E, Guggino WB, and Kottgen M (2009) Identification of a urate transporter, ABCG2, with a common functional polymorphism causing gout. *Proc Natl Acad Sci U S A* **106:**10338-10342.

Wu CP, Shukla S, Calcagno AM, Hall MD, Gottesman MM, and Ambudkar SV (2007) Evidence for dual mode of action of a thiosemicarbazone, NSC73306: a potent substrate of the multidrug resistance linked ABCG2 transporter. *Mol Cancer Ther* **6:**3287-3296.

Zelinski T, Coghlan G, Liu XQ, and Reid ME (2012) ABCG2 null alleles define the Jr(a-) blood group phenotype. *Nat Genet* **44:**131-132.

Zhang S, Wang X, Sagawa K, and Morris ME (2005) Flavonoids chrysin and benzoflavone, potent breast cancer resistance protein inhibitors, have no significant effect on topotecan pharmacokinetics in rats or mdr1a/1b (-/-) mice. *Drug Metab Dispos* **33:**341-348.

Zhang Y, Laterra J, and Pomper MG (2009) Hedgehog pathway inhibitor HhAntag691 is a potent inhibitor of ABCG2/BCRP and ABCB1/Pgp. *Neoplasia* **11:**96-101.

Footnotes

This research was supported by the Intramural Research Program of the National Institutes of Health, National Cancer Institute.

The authors declare no conflicts of interest.

Figure Legends

Fig. 1. Expression of ABCG2 in mouse cell lines determined by Simple Western analysis. The electropherogram (right) and corresponding "virtual blot" image (left) of Simple Western analyses of mouse cell lysates probed for ABCG2, and α-tubulin as an internal loading control. The following mouse cell line pairs are shown: (**A(** 3T3, 3T3 MX15 (ABCG2), (**B)** Ltk- and Ltk-HoeR415 (ABCG2). An increase in ABCG2 expression is observed in the drug-selected 3T3 MX15 and Ltk- HoeR415 (H-415) in respective to their parental lines. ABCG2 normalized to α-tubulin are shown below the virtual blot image.

Fig. 2. Overlapping substrate and inhibitor specificity of human and mouse ABCG2. Substrates and inhibitors demonstrate similar effects with human and mouse ABCG2 as determined by flow cytometry. **(A)** Values from Table 1 (percentage of inhibitable efflux in ABG2-expressing sublines) were averaged for human and mouse ABCG2 efflux and compared. Only rhodamine 123 demonstrated a significant difference in efflux, but this was due to P-gp function in the mouse ABCG2-expressing sublines used. (**B)** Values from Table 2 (fold increase of purpurin-18 accumulation by select inhibitors) were averaged for human and mouse ABCG2. No significant differences were observed.

Fig. 3. Purpurin-18 is a specific substrate of human and mouse ABCG2. (**A)** The structure of Pp-18 (exc: 630 nm, em: 660 nm) is shown. (**B)** Flow cytometry analysis of Pp-18 accumulation in parental (top row) and respective ABCG2-expressing cells (bottom row). Cells incubated without (grey) and with (black) the ABCG2 inhibitor Ko143 (10 μM) are shown for each cell line. (**C)** Flow cytometry analysis of Pp-18 accumulation in human parental (top row) and resistant cell lines that overexpress P-gp (KB-8-5-11) or MRP1 (VP16) (bottom row). No significant

differences in Pp-18 efflux are seen without inhibitors (grey), and the presence of inhibitors (black) of P-gp (verapamil, 20 μM) and MRP1 (indomethacin, INN, 100 μM) have no effect. (**D)** Flow cytometry analysis of Pp-18 accumulation in mouse parental (top row) and resistant cell lines that overexpress P-gp (C3M). No significant differences in Pp-18 efflux are seen without inhibitors (grey), and in the presence of a P-gp inhibitor (black) (verapamil, 20 μM). Values from three independent experiments for each fluorophore examined in this way are shown in Table 1.

Fig. 4. Cyclosporin A inhibits purpurin-18 efflux in ABCG2-expressing cell lines in a dose-dependent manner. A dose-dependent increase in accumulation of Pp-18 when CsA (1, 5, 10, 25, 50 μM) was added to cell with Pp-18 (15 μM). The highest inhibition is demonstrated in the mouse cell lines when CsA was added at 50 μM. Accumulation values are normalized to the accumulation in the presence of Ko143 (10 μM). Data represent means ± S.D. of three observations.

DMD Fast Forward. Published on July 18, 2013 as DOI: 10.1124/dmd.113.053140
This article has not been copyedited and formatted. The final version may differ from this version.

TABLE 1

Ko143-inhibitable efflux of fluorescent compounds in human and mouse ABCG2

			Human ABCG2		Mouse ABCG2	
			H460 MX20	MCF FLV500	3T3 MX15	Ltk- HoeR415
Substrates	Conc.	Exc/Em	Efflux[a] ± SD (%)			
Mitoxantrone[b]	10 μM	630/660	78.3 ± 2.7	70.8 ± 1.5	69.9 ± 3.5	51.6 ± 4.5
Hoechst 33342[b]	1 μM	350/530	86.9 ± 2.3	67.6 ± 1.4	90.0 ± 6.5	52.9 ± 13.7
BODIPY Prazosin[b]	250 nM	488/530	86.8 ± 1.3	77.4 ± 4.2	77.8 ± 3.2	70.4 ± 0.8
Pheophorbide a	10 μM	630/660	85.4 ± 0.6	80.9 ± 6.0	91.4 ± 0.8	46.0 ± 7.9
Pyropheophorbide a methyl ester	10 μM	630/660	90.1 ± 3.1	69.9 ± 1.0	80.5 ± 14	57.9 ± 12.2
Purpurin-18	15 μM	630/660	92.5 ± 1.4	76.7 ± 1.0	67.3 ± 4.7	66.0 ± 10.4
Chlorin e6	50 μM	630/660	84.7 ± 1.6	52.0 ± 5.0	72.2 ± 2.3	48.2 ± 5.5
Daunorubicin[b]	1 μM	488/570	13.1 ± 1.9	17.3 ± 2.9	18.6 ± 11.6	19.6 ± 11.6
Rhodamine123[b]	2 μM	488/530	0	0	21.3 ± 1.1[c]	48.8 ± 2.3[c]

[a]Accumulation is normalized to the fluorescence of cells in each substrate in the presence of Ko143 (10 μM) and the mean percentage difference with and without the inhibitor is recorded. Data represent means ± S.D. of three observations. Negative values were assigned the value of zero.

[b]Also substrates of P-gp.

[c]Due to baseline P-gp efflux.

DMD Fast Forward. Published on July 18, 2013 as DOI: 10.1124/dmd.113.053140
This article has not been copyedited and formatted. The final version may differ from this version.

TABLE 2

Fold-increase of purpurin-18 fluorescence with inhibitors

		Human ABCG2		Mouse ABCG2	
		H460 MX20	MCF FLV500	3T3 MX15	Ltk- HoeR415
Inhibitor	Conc.	Fold[a] ± SD			
Ko143	10 μM	9.00 ± 0.03	5.00 ± 0.04	2.89 ± 0.01	5.69 ± 0.01
Fumitremorgin C	10 μM	8.57 ± 0.03	7.64 ± 0.03	3.45 ± 0.01	4.86 ± 0.01
Elacridar	5 μM	4.62 ± 0.02	3.38 ± 0.02	1.96 ± 0.01	3.73 ± 0.04
Tariquidar	5 μM	5.46 ± 0.04	4.23 ± 0.04	1.74 ± 0.01	4.10 ± 0.02
Nilotinib	5 uM	6.04 ± 0.01	3.88 ± 0.06	2.69 ± 0.13	4.77 ± 0.01
Quercetin	50 μM	6.03 ± 0.04	5.03 ± 0.04	1.53 ± 0.01	2.59 ± 0.02
NSC73306	100 μM	5.10 ± 0.02	3.78 ± 0.05	2.04 ± 0.01	3.27 ± 0.01
Flavoperidol	5 μM	4.09 ± 0.03	1.85 ± 0.02	1.84 ± 0.02	3.90 ± 0.02
Chrysin	50 μM	15.11 ± 0.11	8.73 ± 0.07	4.49 ± 0.02	9.49 ± 0.44
Benzoflavone	5 μM	8.80 ± 0.02	6.34 ± 0.02	4.45 ± 0.09	10.30 ± 0.04
Estradiol	100 μM	8.50 ± 0.02	6.11 ± 0.12	3.37 ± 0.03	5.43 ± 0.07
Novobiocin	100 μM	7.30 ± 0.05	4.67 ± 0.04	2.51 ± 0.01	3.65 ± 0.04
Vismodegib	50 μM	4.09 ± 0.03	3.21 ± 0.01	2.01 ± 0.02	3.47 ± 0.01
Sulfasalazine	100 μM	1.05 ± 0.08	1.03 ± 0.03	1.07 ± 0.01	1.41 ± 0.05

[a]The fold value is defined as the flouresence of Pp-18 in cells in the presence of an inhibitor divided by the accumulation of Pp-18 in the absence of inhibitor. Data represent means ± S.D. of three observations.

DMD Fast Forward. Published on July 18, 2013 as DOI: 10.1124/dmd.113.053140
This article has not been copyedited and formatted. The final version may differ from this version.

Figure 1

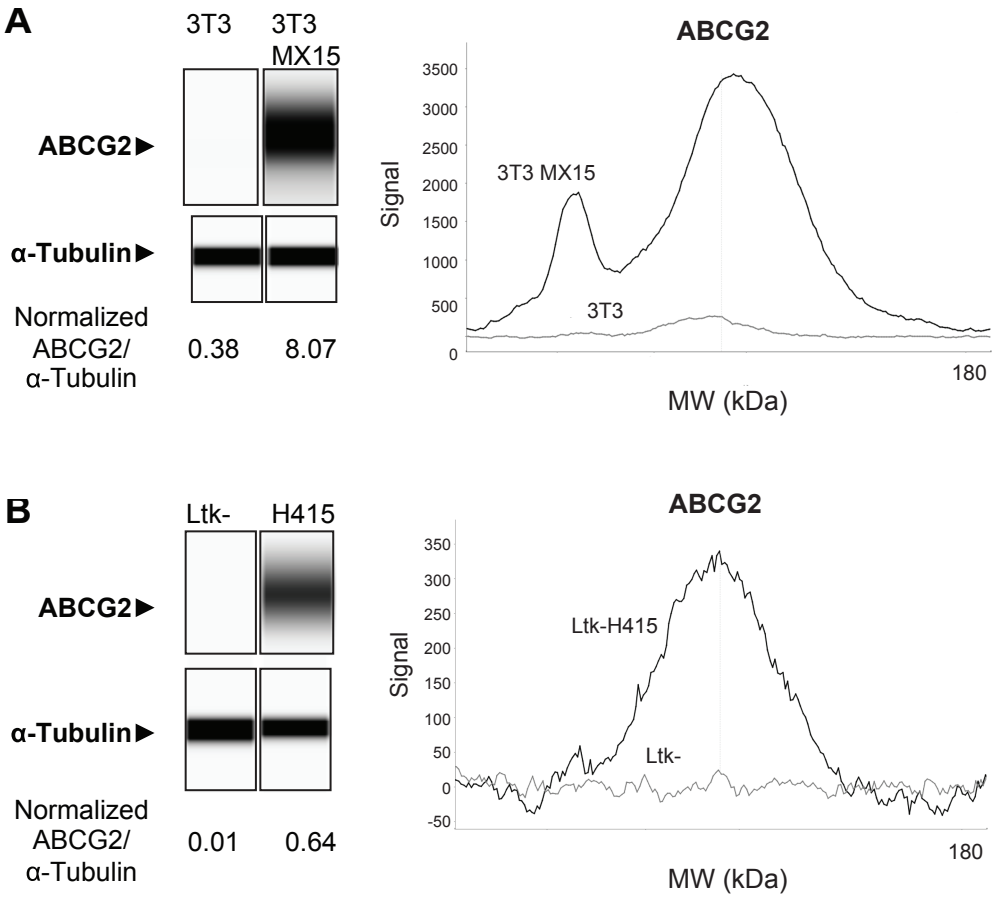

DMD Fast Forward. Published on July 18, 2013 as DOI: 10.1124/dmd.113.053140
This article has not been copyedited and formatted. The final version may differ from this version.

Figure 2

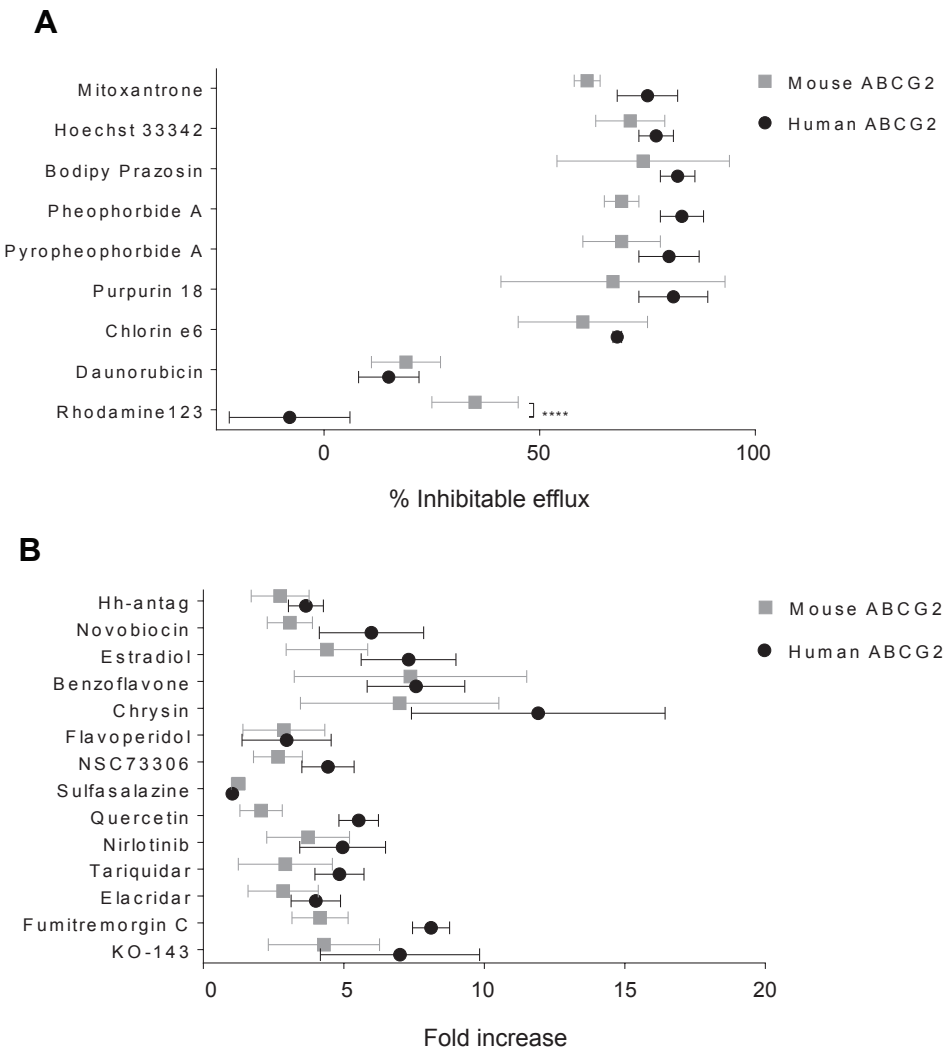

DMD Fast Forward. Published on July 18, 2013 as DOI: 10.1124/dmd.113.053140
This article has not been copyedited and formatted. The final version may differ from this version.

Figure 3

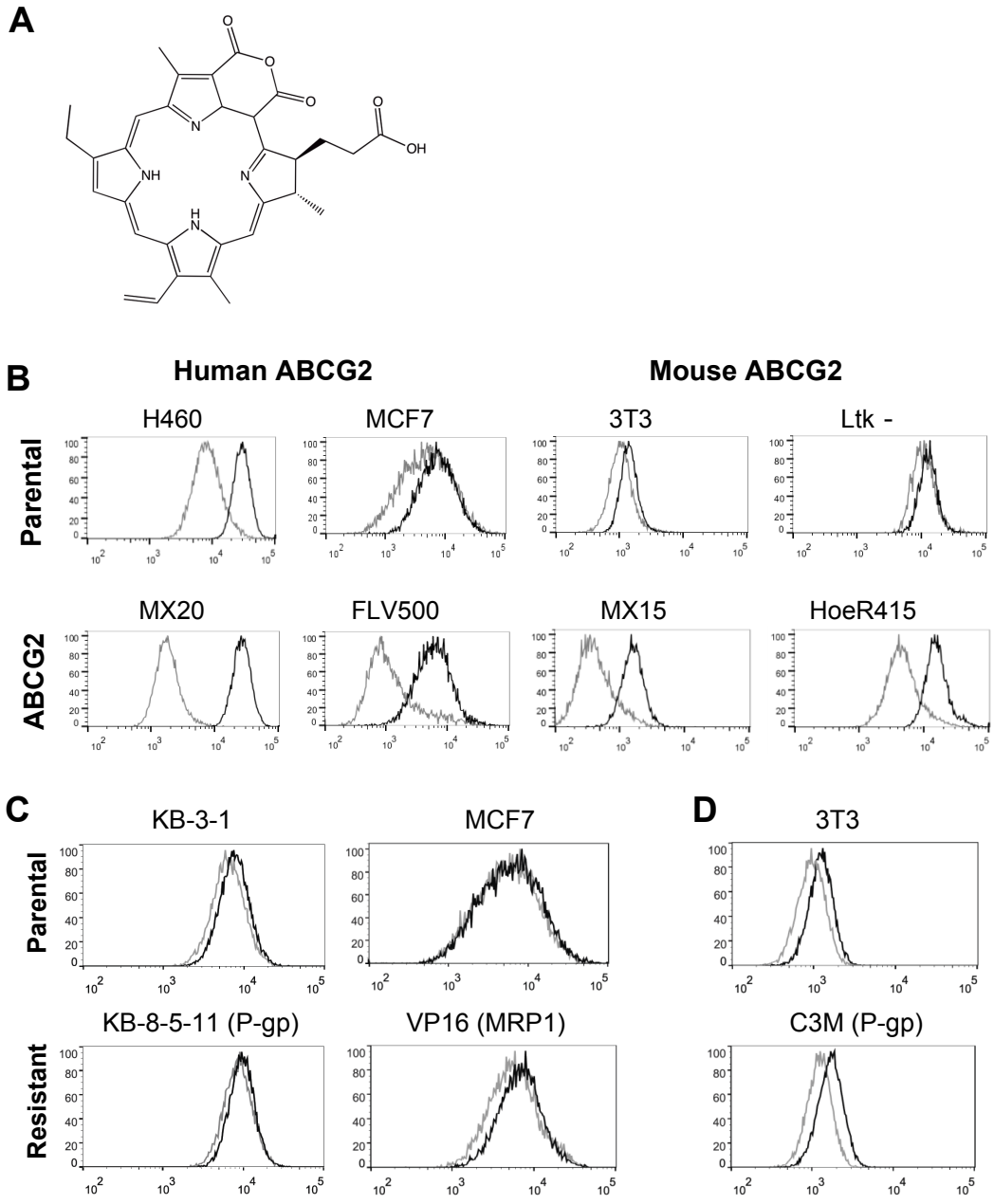

DMD Fast Forward. Published on July 18, 2013 as DOI: 10.1124/dmd.113.053140
This article has not been copyedited and formatted. The final version may differ from this version.

Figure 4

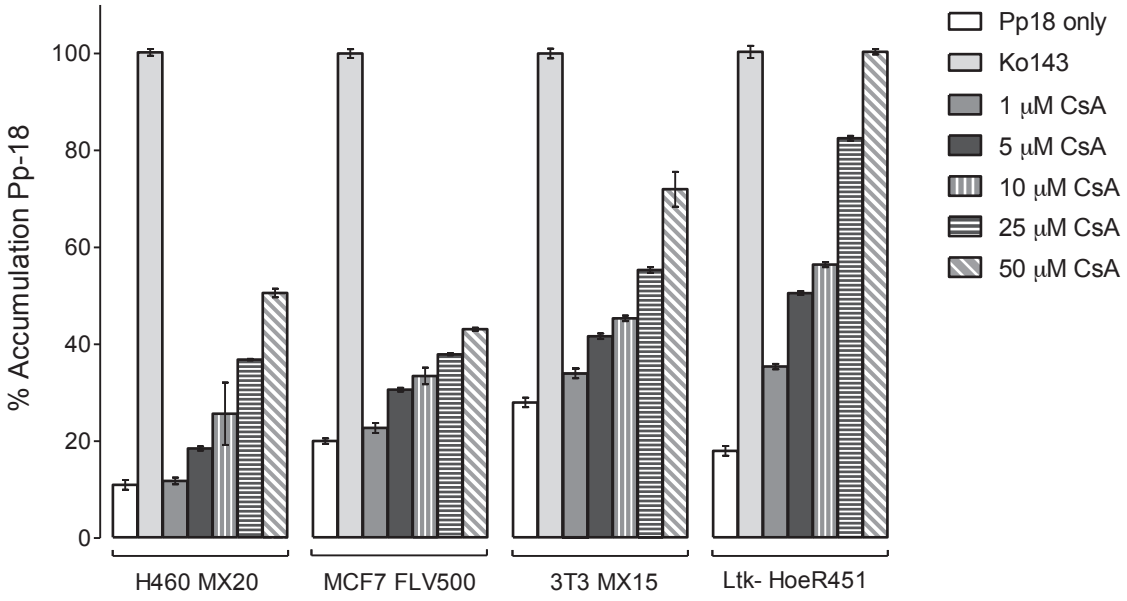

Drug Metabolism and Disposition

Supplemental Figures

Overlapping Substrate and Inhibitor Specificity of Human and Murine ABCG2

Joshua Bakhsheshian, Matthew D. Hall, Robert W. Robey, Michelle A. Herrmann, Jin-Qiu Chen, Susan E. Bates, Michael M. Gottesman

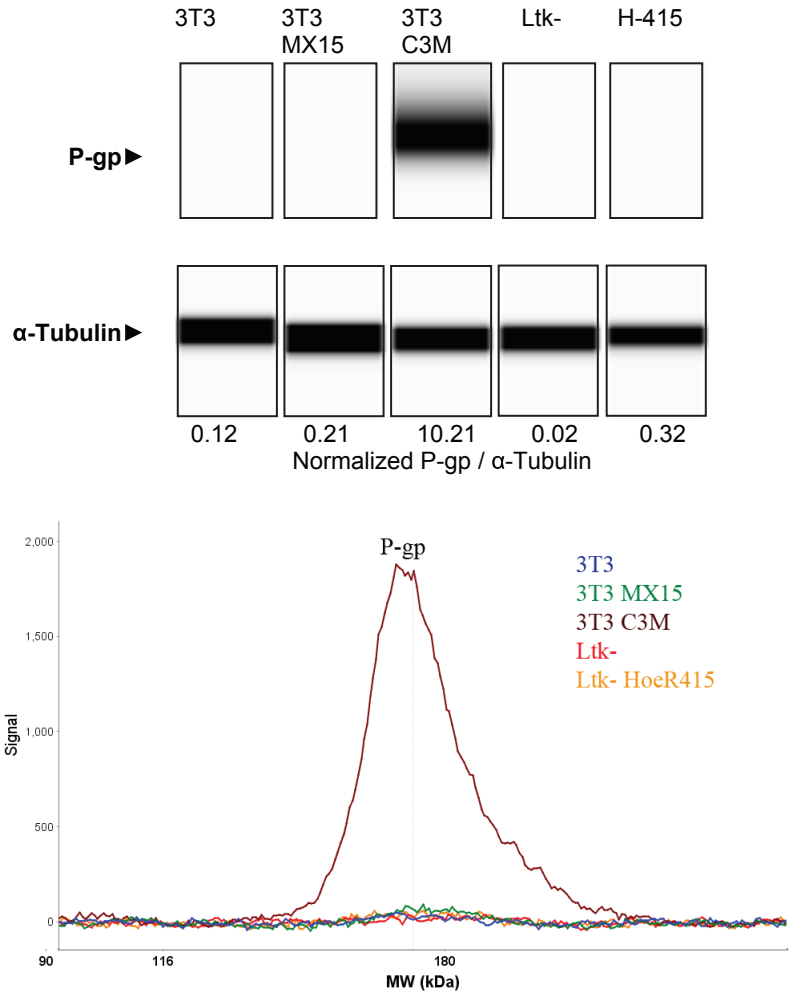

Supplemental Figure 1. Expression of P-gp in mouse cell lines determined by Simple Western analysis. The electropherogram (bottom) and corresponding "virtual blot" image (top) of Simple Western analyses of mouse cell lysates probed for P-gp and α-tubulin as an internal loading control. The following mouse cell line pairs are shown: 3T3, 3T3 MX15 (ABCG2), 3T3 C3M (P-gp), Ltk- and Ltk- HoeR415 (ABCG2). A significant increase in P-gp expression is observed in the drug-selected 3T3 C3M subline. P-gp normalized to α-tubulin are shown below the virtual blot image.

Supplemental Figure 2

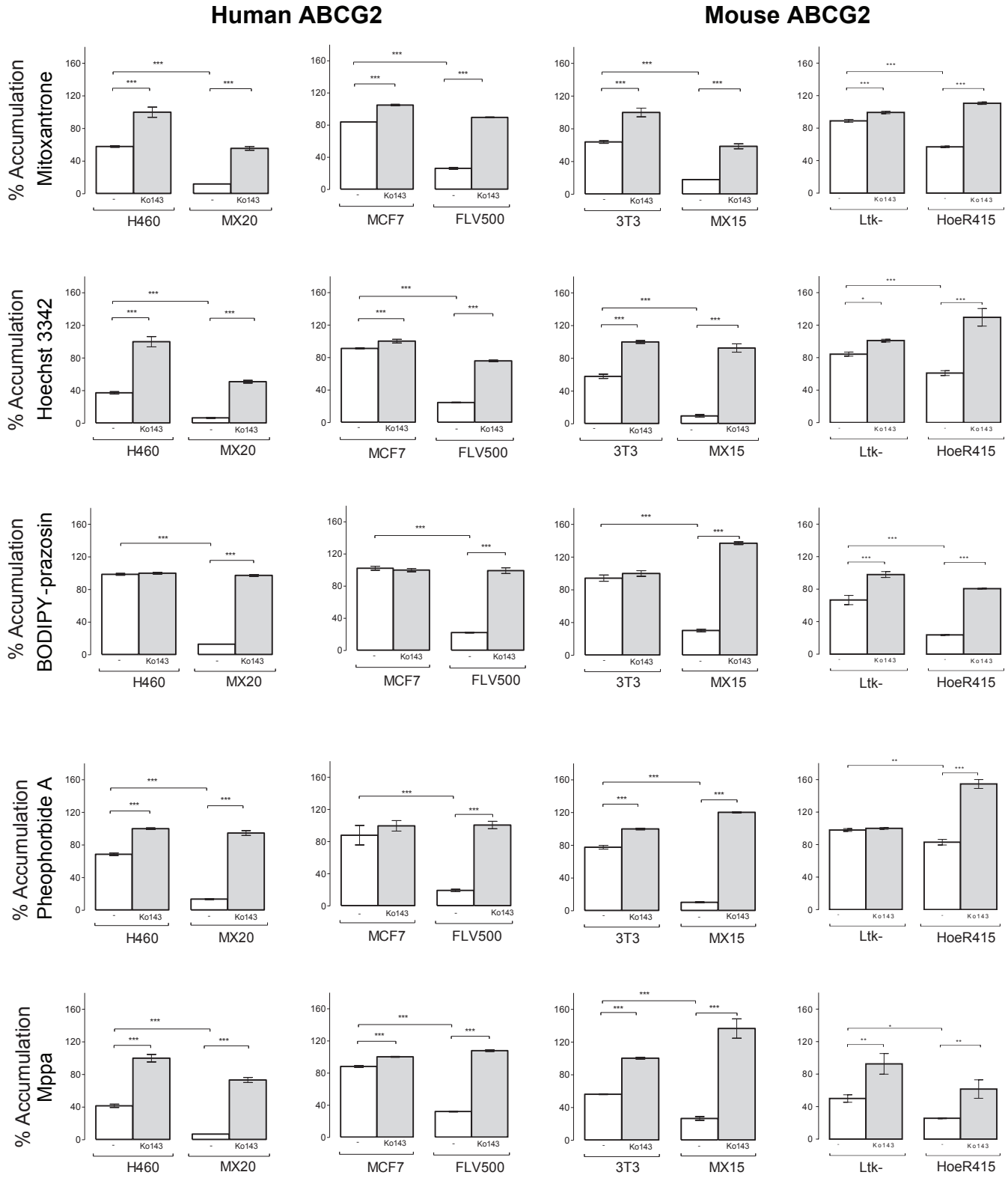

(Continued on next page)

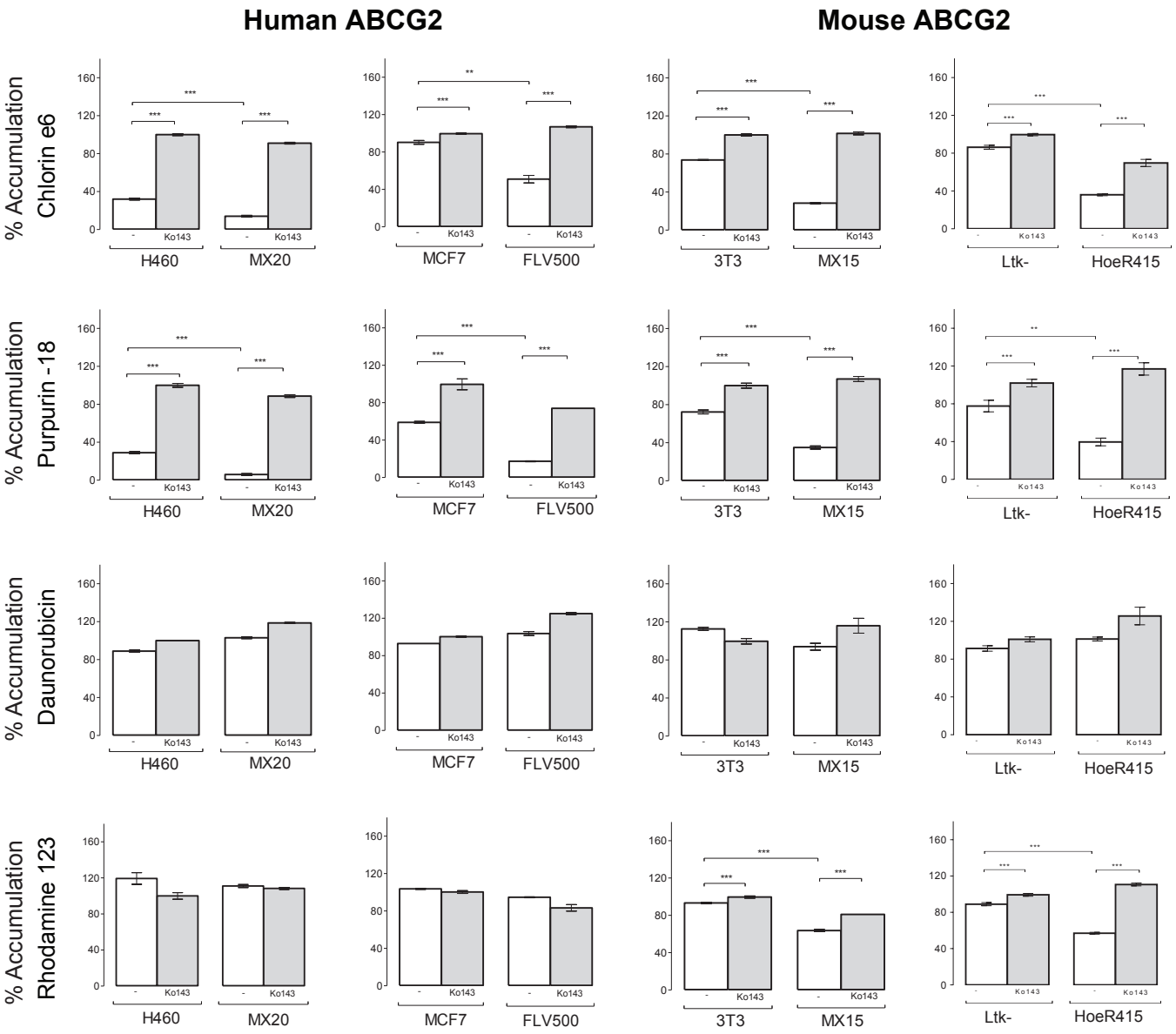

Supplemental Figure 2. Flow cytometry analysis of substrate accumulation in human and mouse parental and ABCG2-expressing cells. The concentrations used and the excitation/emission are listed in Table 1. Mitoxantrone, Hoechst 33342, BODIPY-prazosin, pheophorbide a, MPPa, and chlorin e6 demonstrated a significant efflux in human and mouse ABCG2-expressing cells when compared to parental cells and the accumulation of substrates increased when co-incubated with Ko143. Daunorubicin accumulation did not demonstrate a difference in the parental and ABCG2-expressing cell line with or without Ko143. The efflux of rhodamine 123 in mouse ABCG2-expressing cells is due to low P-gp expression. All accumulation values are normalized to the parental accumulation in the presence of Ko143 (10 μM). Data represent means ± S.D. of three observations ***, $P<0.001$ by a two-way ANOVA followed by the Bonferroni post-t test ($\alpha = 0.05$).

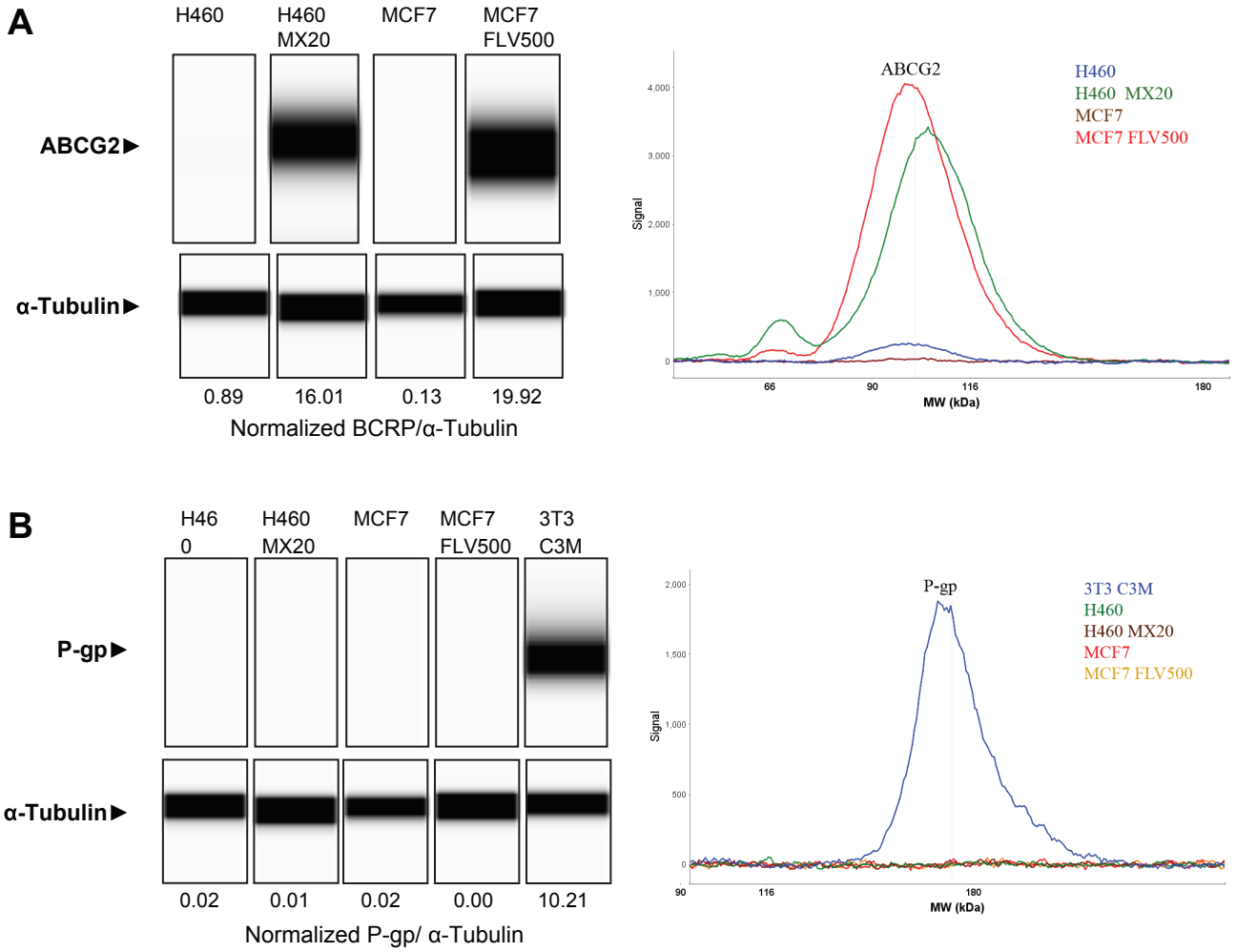

Supplemental Figure 3. Expression of ABCG2 and P-gp in human cell lines determined by Simple Western analysis. The following human cell line pairs are shown: H460, H460 MX20 (ABCG2), MCF7, MCF7 FLV500 (ABCG2) and the mouse cell line 3T3 C3M (P-gp). The electrophoretogram (right) and corresponding "virtual blot" image (left) of Simple Western analyses of mouse cell lysates probed for ABCG2 or P-gp and α-tubulin as an internal loading control. ABCG2 or P-gp normalized to α-tubulin are shown below the virtual blot image.

Cell Line	
3T3	CAGAGGGAGGTCTTCAGGTGCTGGATTGCATAACAGCCAGAGGAACTATTGTAAAGAGAGTGGGC TACAGTCTGAGAGCCTCCTGAAGCTGAGAGCATAGAAGTTGGCCCCTAAGATGGCAGAAGACATG GGGGTCAGCCTGGAGCATGTGGGCGCTGCCTTACTAGAAATCTAGTGGAGCAGCAAGAAACCAAT CTTCTGTTCTGTACCTTTGTAGACTAATGTGGGATCTATGTTCTGTGTTTTTATAG**ACATGAGTACAT** **CAGTGGATATTACAGAGTGTCTTCTTACTTCTTTGGAAAGGTGATGTCTGATTTACTCCCCATG<u>AG</u>** **<u>G</u>TTCTTGCCAAGTGTTATATTCACTTGTATATTATACTTCATGTTA**GGTAAGTAACAGACCAAGTGA AAGTGCCTCTAGTCACAGATGTAAAGTGAAGCTAATTTCTCTGTATATTTCTATTTACCGTTTTCTAA GTGTCTATACAAAGAGATCTAAGAATTTTAATAATTACTCATATTCTAATGTATATTCTTTAGTAAAAA ATATTGGAGGTTTATTTATTTACTAAAAAAAAAATCACAGATTTAATTTTGCATTATCCTCAGGCTTCC ACCTTAGGATCGTGACATCAAAATTTCCAAGTTTTTCACTGATATATGTGCACATGCCTATATACTGT TCTGTTTTTACAAAGCACTGATAGAGCTTTAAAAACTTCCATTTTATATATGTGGTTTTTCATAAAGAA TATGAGAATGGGATCTAGACCCTTAGATTCCTGCCCTATCTTTCTGCC
3T3 MX15	CAGAGGGAGGTCTTCAGGTGCTGGATTGCATAACAGCCAGAGGAACTATTGTAAAGAGAGTGGGC TACAGTCTGAGAGCCTCCTGAAGCTGAGAGCATAGAAGTTGGCCCCTAAGATGGCAGAAGACATG GGGGTCAGCCTGGAGCATGTGGGCGCTGCCTTACTAGAAATCTAGTGGAGCAGCAAGAAACCAAT CTTCTGTTCTGTACCTTTGTAGACTAATGTGGGATCTATGTTCTGTGTTTTTATAG**ACATGAGTACAT** **CAGTGGATATTACAGAGTGTCTTCTTACTTCTTTGGAAAGGTGATGTCTGATTTACTCCCCATG<u>AG</u>** **<u>G</u>TTCTTGCCAAGTGTTATATTCACTTGTATATTATACTTCATGTTA**GGTAAGTAACAGACCAAGTGA AAGTGCCTCTAGTCACAGATGTAAAGTGAAGCTAATTTCTCTGTATATTTCTATTTACCGTTTTCTAA GTGTCTATACAAAGAGATCTAAGAATTTTAATAATTACTCATATTCTAATGTATATTCTTTAGTAAAAA ATATTGGAGGTTTATTTATTTACTAAAAAAAAAATCACAGATTTAATTTTGCATTATCCTCAGGCTTCC ACCTTAGGATCGTGACATCAAAATTTCCAAGTTTTTCACTGATATATGTGCACATGCCTATATACTGT TCTGTTTTTACAAAGCACTGATAGAGCTTTAAAAACTTCCATTTTATATATGTGGTTTTTCATAAAGAA TATGAGAATGGGATCTAGACCCTTAGATTCCTGCCCTATCTTTCTGCC
Ltk-	CAGAGGGAGGTCTTCAGGTGCTGGATTGCATAACAGCCAGAGGAACTATTGTAAAGAGAGTGGGC TACAGTCTGAGAGCCTCCTGAAGCTGAGAGCATAGAAGTTGGCCCCTAAGATGGCAGAAGACATG GGGGTCAGCCTGGAGCATGTGGGCGCTGCCTTACTAGAAATCTAGTGGAGCAGCAAGAAACCAAT CTTCTGTTCTGTACCTTTGTAGACTAATGTGGGATCTATGTTCTGTGTTTTTATAG**ACATGAGTACAT** **CAGTGGATATTACAGAGTGTCTTCTTACTTCTTTGGAAAGGTGATGTCTGATTTACTCCCCATG<u>AG</u>** **<u>G</u>TTCTTGCCAAGTGTTATATTCACTTGTATATTATACTTCATGTTA**GGTAAGTAACAGACCAAGTGA AAGTGCCTCTAGTCACAGATGTAAAGTGAAGCTAATTTCTCTGTATATTTCTATTTACCGTTTTCTAA GTGTCTATACAAAGAGATCTAAGAATTTTAATAATTACTCATATTCTAATGTATATTCTTTAGTAAAAA ATATTGGAGGTTTATTTATTTACTAAAAAAAAAATCACAGATTTAATTTTGCATTATCCTCAGGCTTCC ACCTTAGGATCGTGACATCAAAATTTCCAAGTTTTTCACTGATATATGTGCACATGCCTATATACTGT TCTGTTTTTACAAAGCACTGATAGAGCTTTAAAAACTTCCATTTTATATATGTGGTTTTTCATAAAGAA TATGAGAATGGGATCTAGACCCTTAGATTCCTGCCCTATCTTTCTGCC
Ltk- HoeR415	CAGAGGGAGGTCTTCAGGTGCTGGATTGCATAACAGCCAGAGGAACTATTGTAAAGAGAGTGGGC TACAGTCTGAGAGCCTCCTGAAGCTGAGAGCATAGAAGTTGGCCCCTAAGATGGCAGAAGACATG GGGGTCAGCCTGGAGCATGTGGGCGCTGCCTTACTAGAAATCTAGTGGAGCAGCAAGAAACCAAT CTTCTGTTCTGTACCTTTGTAGACTAATGTGGGATCTATGTTCTGTGTTTTTATAG**ACATGAGTACAT** **CAGTGGATATTACAGAGTGTCTTCTTACTTCTTTGGAAAGGTGATGTCTGATTTACTCCCCATG<u>AG</u>** **<u>G</u>TTCTTGCCAAGTGTTATATTCACTTGTATATTATACTTCATGTTA**GGTAAGTAACAGACCAAGTGA AAGTGCCTCTAGTCACAGATGTAAAGTGAAGCTAATTTCTCTGTATATTTCTATTTACCGTTTTCTAA GTGTCTATACAAAGAGATCTAAGAATTTTAATAATTACTCATATTCTAATGTATATTCTTTAGTAAAAA ATATTGGAGGTTTATTTATTTACTAAAAAAAAAATCACAGATTTAATTTTGCATTATCCTCAGGCTTCC ACCTTAGGATCGTGACATCAAAATTTCCAAGTTTTTCACTGATATATGTGCACATGCCTATATACTGT TCTGTTTTTACAAAGCACTGATAGAGCTTTAAAAACTTCCATTTTATATATGTGGTTTTTCATAAAGAA TATGAGAATGGGATCTAGACCCTTAGATTCCTGCCCTATCTTTCTGCC

Supplemental Figure 4. Sequencing data for 3T3, 3T3 MX15, Ltk- and Ltk- HoeR415 showed wildtype sequence (R482, underlined) with no trace of secondary mutant DNA signatures. Therefore these cell lines are homozygous for wildtype ABCG2 at this position. Genomic DNA for all samples was extracted using the QIAamp DNA Mini Kit (QIAGEN) using manufacturer's conditions, and eluted in 200 µL TE (Tris and EDTA) buffer. PCR samples were set up for each genomic DNA sample using 1 µl of each 5 µM primer stock, 9.5 µL dH2O, and 12.5 µL Phusion HF PCR Master Mix with HF Buffer (NEB). Samples were cycled according to the following conditions: 98 oC 30 sec, (98 oC 10 sec, 65 oC 30 sec, 72 oC 30 sec) x35, 72 oC 10 min. After agarose gel verification, samples were purified using the QIAquick PCR Purification Kit and eluted in 50 µL TE buffer before being sent for sequencing with their PCR primers. Sequencing was performed at the Laboratory of Molecular Technology (LMT) Sanger Sequencing facility. PCR primers used were: Forward: 5'-CAGAGGGAGGTCTTCAGGTG; Reverse: 5'- GGCAGAAAGATAGGGCAGGA.

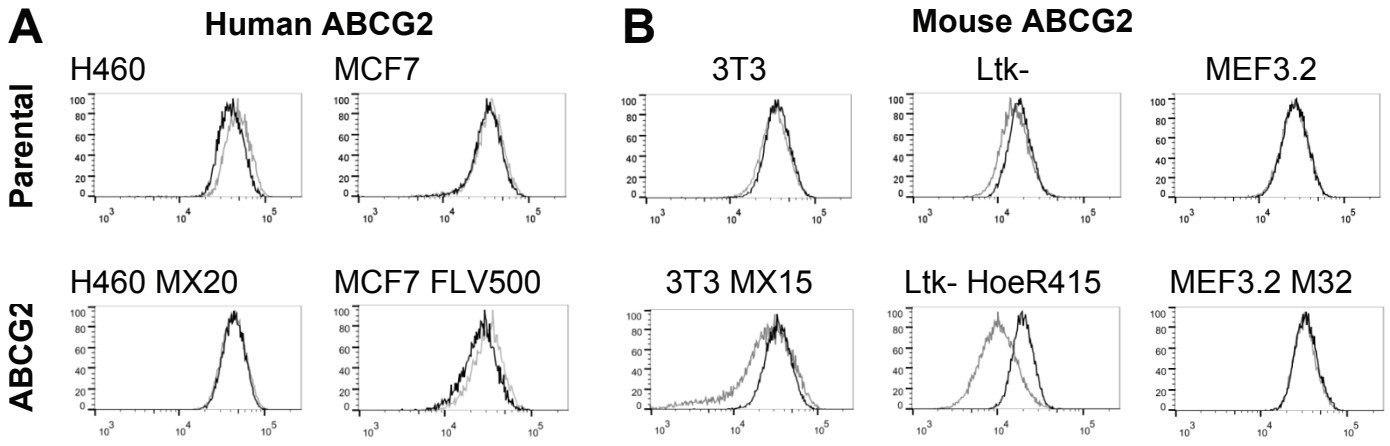

Supplemental Figure 5. Rhodamine 123 is not a mouse ABCG2 substrate. Flow cytometry analysis of rhodamine 123 accumulation in parental and ABCG2-expressing cells. The parental cell lines in the top row; H460 (grey), MCF7 (grey), 3T3 (grey), Ltk- (grey) and MEF3.8 (grey) demonstrate high accumulation of rhodamine 123, and this does not change in the presence of Ko143 (10 μM, black). The human ABCG2-expressing cell lines (grey) in the bottom row do not demonstrate a decrease in rhodamine 123 accumulation and it does not increase in the presence of Ko143 (10 μm). In contrast, two of the mouse ABCG2-expressing cell lines in the bottom row, 3T3 MX15 (grey) and Ltk- HoeR415 (grey) show lower accumulation of rhodamine 123 (represented by a wider peak in 3T3 MX15), and is increased (represented by a narrow peak in 3T3 MX15) in the presence of Ko143 (10 μM, black). However the mouse ABCG2-expressing subline MEF3.8 M32 (derived from Mdr1a/b-/- Mrp1-/-) does not demonstrate a decrease in rhodamine 123 accumulation and does not increase in the presence of Ko143 (10 μm), suggesting the previous observation may be due to an interaction between P-gp and Ko143.

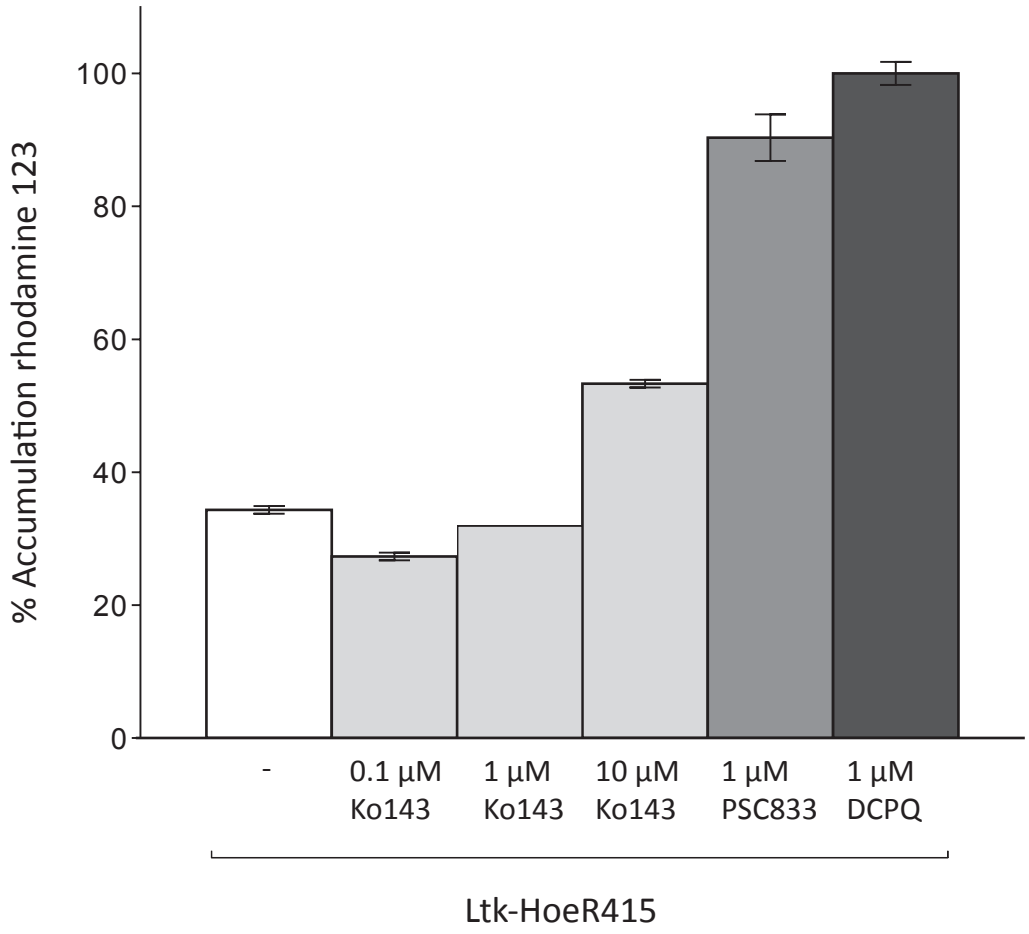

Supplemental Figure 6. Rhodamine 123 efflux in mouse ABCG2-expressing subline is due to P-gp. Flow cytometry data of rhodamine 123 accumulation in Ltk- HoeR415 demonstrated an increase in the presence of Ko143 at high concentrations and P-gp inhibitors (PSC833 and DCPQ). This suggests that rhodamine 123 efflux is due to P-gp and that Ko143 at high concentrations may block some rhodamine 123 efflux. Data represent means ± S.D. of three observations.

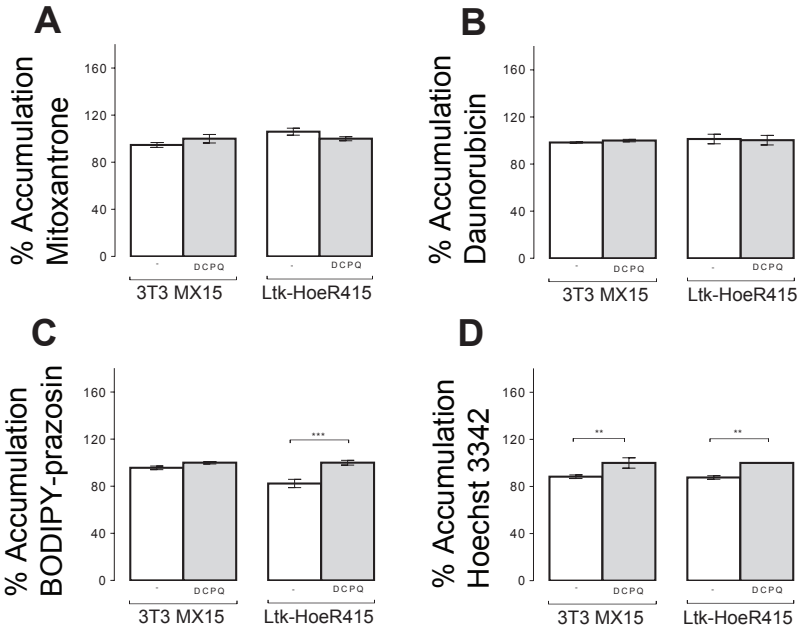

Supplemental Figure 7. Flow cytometry data of known weak substrates of P-gp in mouse ABCG2-expressing subline in the presence of a P-gp inhibitor. Mitoxantrone (10 μM) and daunorubicin (10 μM) accumulation was not different in the presence of DCPQ (1 μM). Hoechst 33342 (1 μM) demonstrated a small but significant difference in the presence of DCPQ and BODIPY-prazosin demonstrated a small but significant difference in the Ltk- HoeR415 cells only. This difference is much smaller when compared to ABCG2 efflux (Supplemental Fig. 2). Data represent means ± S.D. of three observations ***, $P<0.001$ by unpaired Student's two-tailed t test ($\alpha = 0.05$).

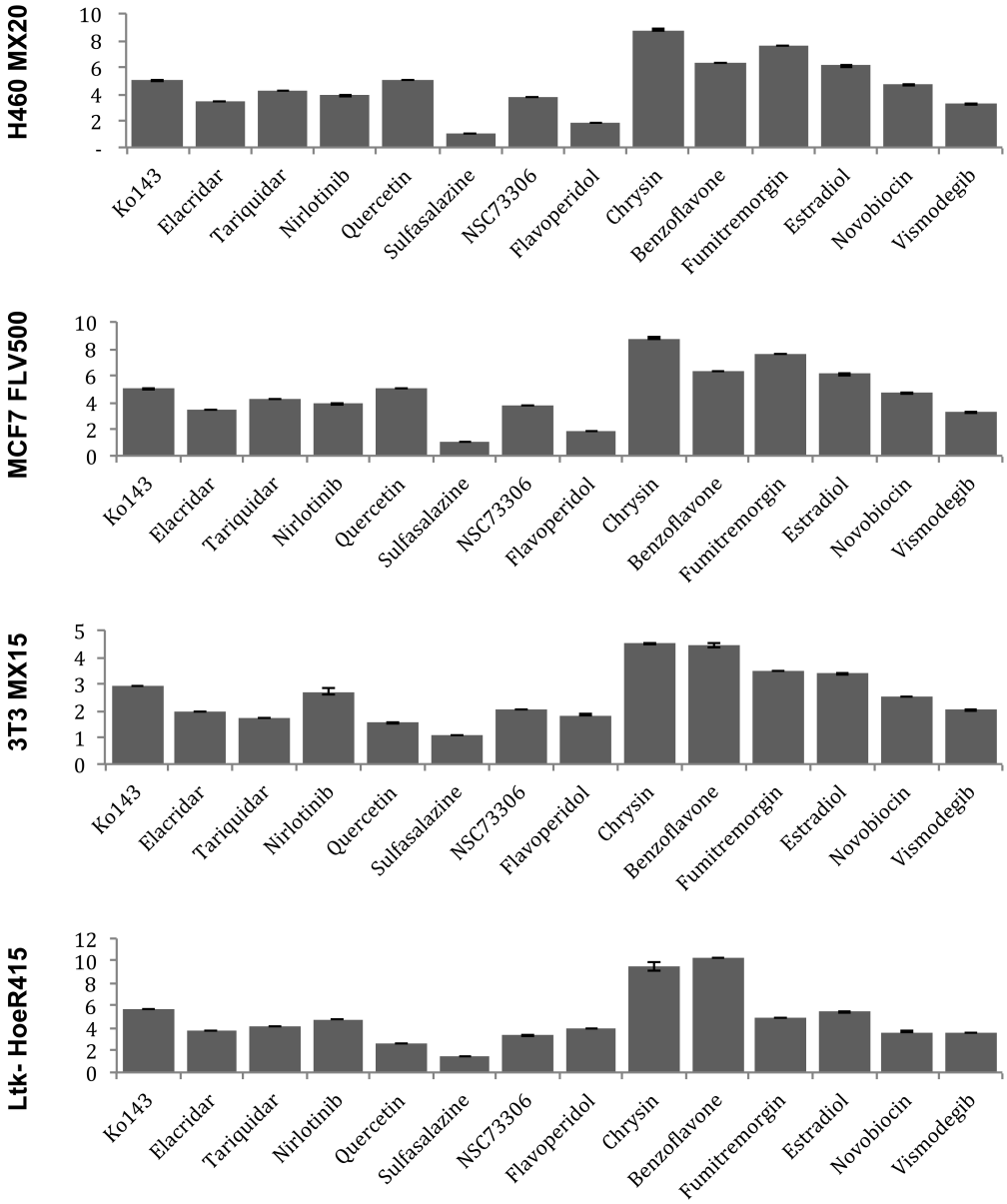

Supplemental Figure 8. Flow cytometry of purpurin-18 accumulation in the presence of the following inhibitors in mouse and human ABCG2-expressing sublines demonstrated a similar pattern of inhibition. The fold value is defined as the accumulation of Pp-18 in the presence of an inhibitor divided by the accumulation of Pp-18 in the absence of any inhibitors. Data represent means ± S.D. of three observations.

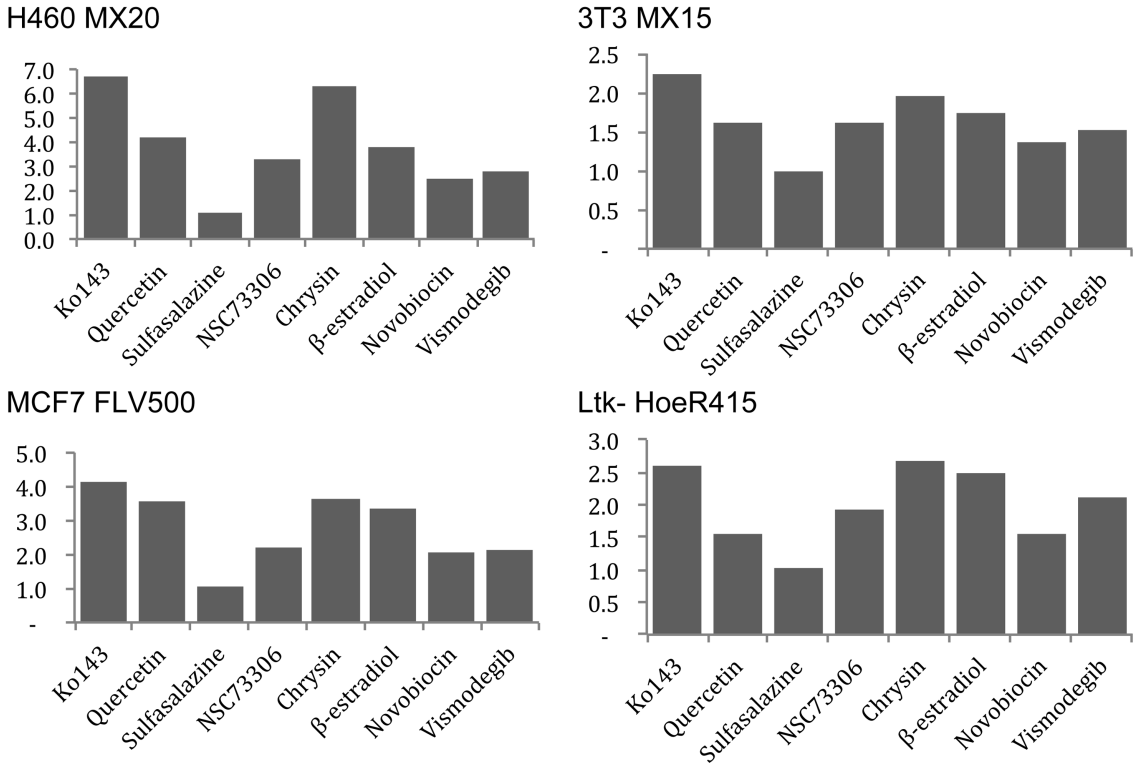

Supplemental Figure 9. Flow cytometry data of pupurin-18 accumulation in the presence of inhibitors at 10 μM demonstrated a similar pattern of inhibition in human and mouse ABCG2-expressing cell lines. The fold value is defined as the accumulation of Pp-18 in the presence of an inhibitor divided by the accumulation of Pp-18 in the absence of any inhibitors.

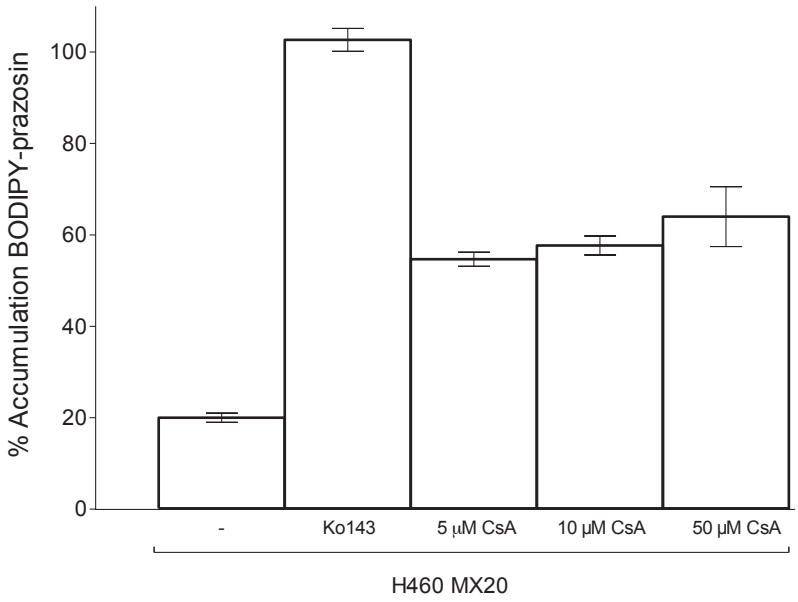

Supplemental Figure 10. Flow cytometry data of BODIPY-prazosin accumulation in the human ABCG2-expressing subline H460 MX20. BODIPY-prazosin accumulation increases in the presence of cyclosporine A (CsA). Data represent means ± S.D. of three observations.